Engineering Structures 141 (2017) 175–183

Contents lists available at ScienceDirect

Engineering Structures

journal homepage: www.elsevier.com/locate/engstruct

Cosine based and extended transmissibility damage indicators for structural damage detection

Yun-Lai Zhou [a], Magd Abdel Wahab [b,c,d,*]

[a] Department of Civil and Environmental Engineering, National University of Singapore, 2 Engineering Drive 2, Singapore 117576, Singapore
[b] Division of Computational Mechanics, Ton Duc Thang University, Ho Chi Minh City, Viet Nam
[c] Faculty of Civil Engineering, Ton Duc Thang University, Ho Chi Minh City, Viet Nam
[d] Soete Laboratory, Faculty of Engineering and Architecture, Ghent University, Technologiepark, Technologiepark Zwijnaarde 903, B-9052 Zwijnaarde, Belgium

ARTICLE INFO

Article history:
Received 15 November 2016
Revised 12 February 2017
Accepted 16 March 2017
Available online 24 March 2017

Keywords:
Structural damage detection
Transmissibility
Modal assurance criterion
Cosine similarity measure

ABSTRACT

Structural damage detection using vibration-based techniques and transmissibility is investigated and proposed with elaborating the mathematical interrelationship between modal assurance criterion (MAC) and cosine similarity measure. From this interrelationship, two new damage indicators, namely cosine based indicator (CI) and extended transmissibility damage indicator (ETDI), are drawn out. Even MAC and cosine similarity measure are normally adopted separately; their kernel agrees well with each other. In this study, we extend these two indicators, derive two new damage indicators, CI and ETDC, and apply them in a transmissibility based structural damage detection technique. In order to verify the feasibility of the developed damage indicators, experimental data for a three-story benchmark structure is adopted. The results from the benchmark demonstrate well performance of both indicators in damage detection, which might imply their potential applicability in further real engineering structures.

1. Introduction

Structural health monitoring (SHM) has undergone booming advancement during the last decades with numerous techniques raised and applied in real engineering projects in both time and frequency domain, empirically based and model methods. For vibration-based techniques, the reader may refer to [1,2], where in [1], vibration-based approaches were summarized and in [2], the survey mainly illustrated the vibration-based techniques in composite structures. Note that this survey also followed the structural damage identification philosophy that damage detection could be considered as a statistical pattern recognition paradigm, which summarized SHM into a four step paradigm: (1) Operational Evaluation; (2) Data Acquisition, Fusion, and Cleansing; (3) Feature Extraction and Information Condensation and (4) Statistical Mode Development for Feature Discrimination. For more details about this paradigm, the reader may refer to [1].

SHM development can be summarized into two main parts: a) testing and measuring techniques and b) methodologies for the measured data interpretation. As to the testing and measuring techniques, along with the history, SHM underwent various techniques such as oil penetrating, modal testing, acoustic emission, ultrasonic testing, eddy current and magnetic particle testing. On the other hand, methodologies like probabilistic based, pattern recognition based, and so on, are also developed to interpret the measured data such as strain based and impedance based. Even more options exist nowadays for SHM, vibration based techniques [3–7] still hold an essential role since its easy conduction but effective and efficient in SHM in both civil engineering and mechanical engineering.

Modal testing and modal analysis serve as the fundamental in vibration-based techniques, which also underwent two main phases: a) experimental modal analysis (EMA) and b) operational modal analysis (OMA). EMA frequently makes use of laboratory testing of specimens to extract modal parameters, such as natural frequencies, mode shapes and Frequency Response Functions (FRFs) in order to avoid the operating conditions. The drawbacks of this method are obvious as it might be convenient for small specimens, while for heavy, large structures such as wind turbines, dam and so on, it will be definitely challenging, or in some cases impossible. Another shortcoming is the cost that the laboratory testing needs to transfer the specimen from operating condition into prototype. This cost includes the reinstallation, dismantling, transferring, testing, which will impose more expenses and does not make the method a cost-effective approach. The OMA tries to

* Corresponding author at: Division of Computational Mechanics, Ton Duc Thang University, Ho Chi Minh City, Viet Nam.
E-mail addresses: magd.abdelwahab@tdt.edu.vn, magd.abdelwahab@ugent.be (M. Abdel Wahab).

http://dx.doi.org/10.1016/j.engstruct.2017.03.030
0141-0296/

avoid these drawbacks by directly testing and analyze the measured responses. Generally speaking, statistical based methods will be taken into consideration for this kind of analysis since the unknown loads shall restrict the analysis to be responses based.

Among all output-based techniques, transmissibility, one concept raised several decades ago, has served as an essential feature in system identification, damage identification, i.e. detection, localization, and quantification. For details about transmissibility, the reader may refer to [8–12]. The transmissibility was elaborated in theoretical advancement perspective in [8,9] by addressing the force transmissibility, direct transmissibility and certain applications. The study in [10] focused on the damage detection historical development with transmissibility by generally summarizing the key investigations during last decades. In [11], transmissibility was reviewed in a general perspective from both theoretical process and engineering applications, while in [12], a concept of transmissibility selection was presented in order to reduce the computation expenses, but simultaneously maintaining the capacity of detecting damage effectively with elaborating the historical development of transmissibility theory and application in a condensed view. In addition to the development of transmissibility theory, vibration based SHM techniques are summarized into two categories, namely physical model and data/statistical model. The physical model based techniques require the physical model as prior in order to have a better analysis with Finite Element Analysis (FEA), while the data model based techniques try to identify damages according to the structural responses under operating/testing condition.

Modal assurance criterion (MAC), firstly raised in late 1970s [13,14], has served as one essential indicator in the later damage detection history. MAC, initially designed for correlation analysis [13–16], has been widely applied to discriminate the damage features from baseline [12,17–25]. The key idea is to construct a damage sensitive feature and to use data analysis tools, to develop damage indicators using MAC [12,17–26] or artificial neural networks (ANNs) [27] to discriminate the current structural pattern from the baseline. On the one hand, different indicators were constructed, such as Frequency Domain Assurance Criterion (FDAC) to analyze the correlation between the analytically calculated and the experimentally measured FRF [15]. This indicator, FDAC, later extended to a particular form known as Response Vector Assurance Criterion (RVAC) intending to measure the correlation between operational deflection shapes [16]. Several years later, by averaging RVAC, Detection and Relative Damage Quantification Indicator (DRQ) was built to detect and quantify the damage relatively [17,19]. Henceforth, DRQ was extended to transmissibility based damage detection and quantification [23]. In [28], the frequency band selection was pointed out that the noise-contaminated band should be avoided in order to reduce the influence in final results. In [21], MAC was applied to the vector of inverse delta transmissibilities for identifying the damage. Similar application also was presented in [22] for transmissibility coherence, compressed transmissibility [12], transmissibility based distance measure [24]. In [25], coordinate modal assurance criterion (COMAC) was utilized to detect damage for a helicopter composite main rotor blade. In addition, MAC was also applied to build objective function in multi-objective framework based damage localization and quantification [18,20], where analytical and experimental flexibilities were taken into consideration.

With regard to cosine similarity measure, which was raised decades ago, it was defined as the inner product of two vectors divided by the product of their lengths [29], expressing the angle between these two vectors. Cosine similarity measure has been applied in various engineering applications [30–35], such as in pattern recognition [30], image recognition [32], neutrosophic sets medical diagnosis [33] and damage identification [31,34,35]. In [31], cosine similarity measure was taken for comparison with other distance measures like Euclidean distance, Manhattan distance, L-infinity, Mahalanobis distance in K-nearest neighbor (KNN) classification method and was applied to Z-24 bridge data sets as case study. This study revealed that similarity measures have significant impact on the pattern recognition success rate. Furthermore, in Refs [34,35] cosine similarity measure was applied to the transmissibility compressed by principal component analysis (PCA) in damage recognition, where it showed well performance in identifying the damages.

Even though MAC and cosine similarity measure have been separately utilized in the past, it might be beneficial for researchers to point out the inter-connection between them. This study aims to unveil the inter-connection between MAC and cosine similarity measure, and thus to propose a comparison between them and some previously developed indicators for transmissibility based damage detection methodology. The remaining sections of the paper are summarized as follows. Section 2 gives the fundamentals of transmissibility, MAC and cosine similarity measure. In Section 3, the damage detection paradigm using transmissibility is presented. Section 4 utilizes experimental data of three-story benchmark structure as case study. Finally concluding remarks are summarized in Section 5.

2. Theoretical fundamentals

2.1. Transmissibility fundamentals

Transmissibility serves as an essential feature for damage detection [8–12,23,26,36,37] as it does not require the measurement of forces, and thus leading to a wide application, and integration with other methods. Transmissibility, generally, is defined as the ratio between two dynamic outputs, and for a linear multiple-degree-of-freedom (MDOF) system subjected to a harmonic loading at a given position, it will be expressed as:

$$T_{(i,j)}(\omega) = \frac{X_i(\omega)}{X_j(\omega)} \tag{1}$$

where X_i and X_j are the complex amplitudes of the system responses, $x_i(t)$ and $x_j(t)$, respectively, and ω is the frequency. In this study, Fourier transform is adopted in obtaining the response spectrum. Certainly Laplace transform can also be adopted, the final detected results will be the same.

Transmissibility can be estimated by several approaches, for instance, directly using the two outputs. In addition, one can also use FRFs if available, or taking average by using auto- and spectra:

$$T_{(i,j)}(\omega) = \frac{X_i(\omega)}{X_j(\omega)} = \frac{X_i(\omega) \times X_i(\omega)}{X_j(\omega) \times X_i(\omega)} = \frac{G_{(i,i)}(\omega)}{G_{(j,i)}(\omega)} \tag{2}$$

where G means the auto- or cross-spectrum. Note that by analog of coherence estimation in FRFs, transmissibility coherence (TC) can be drawn out. For details, the reader may refer to [11,22], where TC is systematically discussed and applied in damage detection and quantification, especially for small nonlinearity quantification. Herein in this study, transmissibility is derived by Eq. (2).

2.2. Modal assurance criterion (MAC)

MAC is normally defined with some vectors, like FRFs, transmissibility and so on. For a general case, e.g. two vectors (two columns), **A** and **B**, it can be expressed as:

$$MAC(\mathbf{A},\mathbf{B}) = \frac{(\mathbf{A}^{\mathrm{T}}\mathbf{B})^2}{(\mathbf{A}^{\mathrm{T}}\mathbf{A})(\mathbf{B}^{\mathrm{T}}\mathbf{B})} \tag{3}$$

where MAC $\in[0,1]$, $()^T$ means the transpose. Note that this will be the same in all equations discussed hereinafter. Furthermore, when MAC equals to '0', it means no correlation between **A** and **B**, while when MAC equals to '1', it means the highest correlation between **A** and **B** takes place [25].

2.3. Cosine similarity measure

Cosine similarity measure aims to illustrate the angle between two vectors, **A** and **B**, and it is expressed as:

$$Cos(\mathbf{A},\mathbf{B}) = \frac{\mathbf{A}^T\mathbf{B}}{|\mathbf{A}||\mathbf{B}|} \tag{4}$$

where Cos $\in[-1, 1]$. When Cos equals to '1', it means that **A** and **B** hold the same direction, while '−1' means that **A** and **B** hold the opposite direction. A clear description for the angle is depicted in Fig. 1.

2.4. Interrelation between MAC and cosine similarity measure

In order to demonstrate the interrelation between MAC and cosine similarity measure, it is better to calculate the square of cosine measure. As expressed in Eq. (5), it is proved that the square of cosine measure is MAC:

$$Cos(\mathbf{A},\mathbf{B})^2 = \left(\frac{\mathbf{A}^T\mathbf{B}}{|\mathbf{A}||\mathbf{B}|}\right)^2 = \frac{(\mathbf{A}^T\mathbf{B})^2}{(\mathbf{A}^T\mathbf{A})(\mathbf{B}^T\mathbf{B})} = MAC(\mathbf{A},\mathbf{B}) \tag{5}$$

From Eq. (5), it is possible to explain why MAC $\in[0,1]$, i.e. the reason is that Cos$\in[-1, 1]$. And this argument could also explain that why '1 – MAC' can be objective function in [18,20], since 1-MAC will be sine^2, which also hold the value $\in[0, 1]$. In addition, using the same argument can explain why as damage increases, MAC does not harmonically increases [21].

Taking α as the angle between two vectors **A** and **B**, then $\alpha \in[0, 2\pi]$ and the MAC indicator have three tendency changing points, namely '$\pi/2$', 'π', '$3\pi/2$'. MAC does not decrease harmonically versus the increase of angle between the two vectors since these three tendency changing points will act as critical values between two tendencies. For instance, when the angle increase from '0' to '$\pi/2$', MAC will decrease from '1' to '0', and from '$\pi/2$' to 'π', MAC will increase from '0' to '1'. Therefore, in this study, '$\pi/2$' is called tendency changing point. Note that since the angle between the two vectors hold $[0, 2\pi]$, then cosine will solely have one tendency changing point at π, then from '0' to 'π', cosine measure decreases from '1' to '−1' harmonically versus the increase of angle between two vectors. While it increases from '−1' to '1' versus the increase of angle between two vectors from 'π' to '2π'. Regarding pattern recognition, all patterns will be recognized from the baseline, namely if the angle between the current pattern and the baseline exists, then it will be identified. Note that the angle 'π' theoretically speaking, will be impossible to see in MAC as MAC = 1, while cosine similarity can figure it out as it is '−1'.

Another point is that if considering cosine similarity measure as power one of cosine, then MAC will be power two of cosine. Thus, taking the absolute value of cosine similarity measure as basis, theoretically speaking, one can define a higher power of cosine as indicator, for instance, power of order R (a constant number), then the new indicator will be depicted as:

$$CI(\mathbf{A},\mathbf{B}) = \left(\left|\frac{\mathbf{A}^T\mathbf{B}}{|\mathbf{A}||\mathbf{B}|}\right|\right)^R = MAC(\mathbf{A},\mathbf{B})^{R/2} \tag{6}$$

where CI represents the cosine based indicator, CI$\in[0, 1]$. Then, comparing with MAC, CI will be more sensitive to damage or noise if choosing a higher R. Thus, the larger the R, the more sensitive the CI to damage. In order to show this point, Fig. 2 draws four lines with the same basis of CI (R = 1) in the margin [0, 1], and one can see that as the power (R) increases from 1, 2, 4 and 8, the values of CI decrease quicker for the ones with higher power in $[0, \pi/2]$, and increase slower in $[\pi/2, \pi]$. This means the higher the power R is, the more sensitivity the CI holds.

2.5. Distance measure

Apart from cosine similarity measure, distance measure can also be adopted to estimate the similarity/dissimilarity between two metrics. Since the key of similarity/dissimilarity measure just tries to recognize the current pattern from a baseline one, this gives the potential to employ any distance measure to estimate. And to SHM, distance metric is the fundamental for any comparison analysis, which serves as the kernel for SHM, where it intends to identify the damages via the difference between the current patterns (under damaged/operating condition) from the baseline (normally means undamaged condition) [11,34–36,38,39].

Unlike MAC and cosine similarity measure intending to assess the angle between baseline and the current pattern, distance measure is also widely applied in pattern recognition, or even in almost all engineering projects and our daily lives, for instance Euclidean distance. Table 1 summarizes the distances commonly used for assessing the distance between vectors both in angles and in quantity, where city block distance, Euclidean distance, Chebyshev distance, Minkowski distance, Mahalanobis distance, Hausdorff distance and MAC, cosine measure and sine measure are included. These measures have been applied in damage detection, and reveal well performance in identifying the damages.

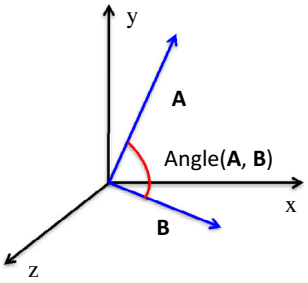

Fig. 1. The angle between vector **A** and **B** measured by cosine similarity measure.

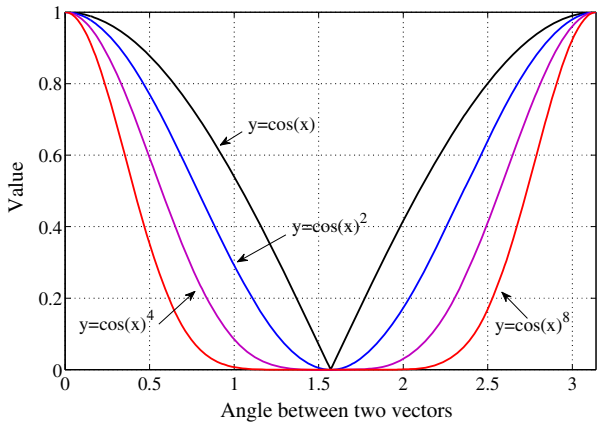

Fig. 2. The influence of power R within a certain margin.

Table 1
Summary for distance measure between vectors.

Distance between vectors No.	Quantitative distance	Angle distance
1	City block distance [12]	Cosine measure [34,35]
2	Euclidean distance [36]	Sine measure
3	Chebyshev distance [12]	MAC [12–14,23,28]
4	Minkowski distance [12,35]	
5	Mahalanobis distance [12,36]	
6	Hausdorff distance [34]	

3. Damage detection methodology

For damage detection, as discussed above, the general procedure is to construct damage sensitive indicators, which will be further employed to identify damages. Certainly kinds of sensitive indicators may be constructed, however, the commonest one will still be MAC, cosine similarity measure and so on. For two data sets $\mathbf{T^u}$ and $\mathbf{T^d}$ representing transmissibility under undamaged state and damaged state, then corresponding damage indicators can be calculated as follows:

3.1. MAC

$$MAC(\mathbf{T^d},\mathbf{T^u}) = \frac{\left((\mathbf{T^d})^{\mathrm{T}}(\mathbf{T^u})\right)^2}{((\mathbf{T^d})^{\mathrm{T}}(\mathbf{T^d}))\left((\mathbf{T^u})^{\mathrm{T}}(\mathbf{T^u})\right)} \tag{7}$$

3.2. Cosine similarity measure

$$Cos\left(\mathbf{T^d},\mathbf{T^u}\right) = \frac{\left(\mathbf{T^d}\right)^{\mathrm{T}}(\mathbf{T^u})}{\left|\mathbf{T^d}\right|\left|\mathbf{T^u}\right|} \tag{8}$$

Note that Cos∈[−1, 1], for damage detection, since the idea is only to discriminate the damaged patterns from the baseline, it will be sufficient to use the absolute value of cosine measure. And certainly, theoretically speaking, MAC will fail to detect the case if the cosine measure equals to '−1', i.e. the two vectors are in opposite direction, as in this case, MAC will also hold the value '1' considering the state to be undamaged as illustrated previously. For engineering application, changing the segment of data sets can solve this. Then, it will be possible to compare MAC and Cosine based indicator (CI), which is expressed as:

$$CI(\mathbf{T^d},\mathbf{T^u}) = \left|\frac{(\mathbf{T^d})^{\mathrm{T}}(\mathbf{T^u})}{|\mathbf{T^d}||\mathbf{T^u}|}\right|^R = MAC(\mathbf{T^d},\mathbf{T^u})^{R/2} \tag{9}$$

where CI∈[0, 1]. One may select different R values for checking the sensitivity of CI in damage detection in comparison to MAC and Cos.

Another indicator based on MAC is illustrated as transmissibility damage indicator (TDI) [23], which is defined as:

$$TDI_m = \frac{1}{N_k}\sum_{k=1}^{N_k}\frac{\left|\sum_{i=1}^{N_i}\sum_{j=1}^{N_j}T_{ij}^m(k\Delta\omega)T_{ij}^r(k\Delta\omega)^T\right|^2}{\left(\sum_{i=1}^{N_i}\sum_{j=1}^{N_j}T_{ij}^m(k\Delta\omega)T_{ij}^m(k\Delta\omega_s)^T\right)\left(\sum_{i=1}^{N_i}\sum_{j=1}^{N_j}T_{ij}^r(k\Delta\omega)T_{ij}^r(k\Delta\omega_s)^T\right)} \tag{10}$$

where m represents mth measurement, $\Delta\omega$ means the frequency resolution, k means the frequency index, N_k, N_i, N_j are the number of frequency lines of the transmissibility, number of coordinates measured and number of excitations measured, respectively [23]. $()^r$ means the reference measured data, i.e. the data measured under undamaged condition.

By analog of the CI definition, one may also extend TDI (ETDI) definition into a general one, which can be illustrated as:

$$ETDI_m = \frac{1}{N_k}\sum_{k=1}^{N_k}\frac{\left|\sum_{i=1}^{N_i}\sum_{j=1}^{N_j}T_{ij}^m(k\Delta\omega)T_{ij}^r(k\Delta\omega)^T\right|^Q}{\left(\left(\sum_{i=1}^{N_i}\sum_{j=1}^{N_j}T_{ij}^m(k\Delta\omega)T_{ij}^m(k\Delta\omega)^T\right)\left(\sum_{i=1}^{N_i}\sum_{j=1}^{N_j}T_{ij}^r(k\Delta\omega)T_{ij}^r(k\Delta\omega)^T\right)\right)^{Q/2}} \tag{11}$$

where Q means the power of TDI. And $Q = 1$ means cosine based TDI; $Q = 2$ means TDI; $Q = 3$ means enhanced TDI, where the sensitivity of ETDI will be higher than TDI. The higher the Q value is, the more sensitive the ETDI will be. Note this is an empirical setting of R and Q relying on the engineer's experience.

Note that FRFs have been commonly used in previous investigations for damage detection. In this study, FRFs are also employed in CI and ETDI indicators for comparison with transmissibility based CI and ETDI.

The damage detection procedure can be illustrated in a three-step paradigm.

Step 1: Transmissibility estimation. In this step, transmissibility will be estimated from structural dynamic responses using Eq. (2);
Step 2: Damage indicators derivation. From Eqs. (10) and (11) damage indicators will be derived;
Step 3: Damage prediction. Finally, one may predict the damages from the results of the indicators in accordance to engineers' experience.

4. Experimental validation

4.1. Model description

In order to verify the developed damage detection procedure and the two newly developed damage indicators, an open source of three-story floor structure tested in Los Alamos Lab is adopted [11,22,40–43] as shown in Fig. 3. The data can be downloaded from (http://www.lanl.gov/projects/national-security-education-center/engineering/ei-software-download/thanks.php). The reason to adopt this structure as a case study is that it has been well investigated in previous work [11,22,40–43], and proves to be a representative structural model in real engineering. Four aluminum columns ($17.7 \times 2.5 \times 0.6\ cm^3$) are adopted to connect the above and below aluminum plates ($30.5 \times 30.5 \times 2.5\ cm^3$). The structure is installed on rails allowing solely x-direction movement. A center column from the top floor is designed to generate nonlinearity when it hits the bumper. A shaker at the center of the base floor excites the structure. Four accelerometers (Channels 2–5) are used to record the horizontal movement of each floor from base, first, second and third floor, and load cell (Channel 1) is adopted to record the excitation. All the time-domain series are measured for 17 different structural conditions as described in Table 2, where for each state, 50 measurements are recorded separately. Further information about this experiment, the reader may refer to [11,22,40–43], all information including the experiment description illustrated above can be found.

4.2. Results and discussion

Results for the proposed damage detection procedure and the newly derived damage indicators, are given and discussed in details hereinafter.

4.2.1. Applicability of transmissibility in damage detection

Figs. 4 and 5 illustrate the transmissibility T(5, 3) and T(4, 3) for the State #1, #2, #6 and #10, respectively. Note here T(5, 3) means

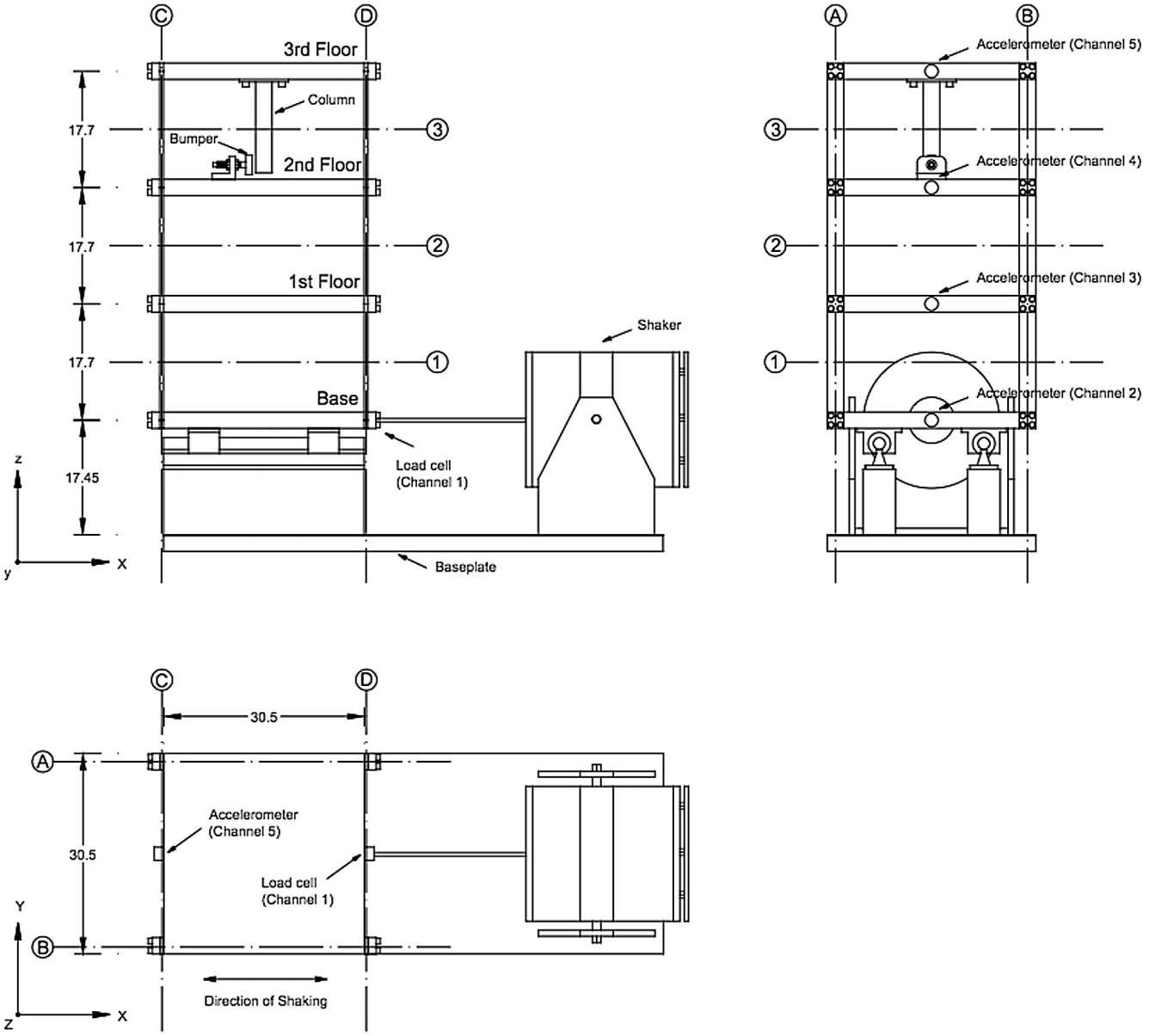

Fig. 3. Schematic diagram of the full test structure [40].

the transmissibility between the measured data from channel 5 (horizontal movement of third floor) and channel 3 (horizontal movement of first floor), and T(4, 3) means transmissibility between channel 4 (horizontal movement of second floor) and channel 3 (horizontal movement of second floor). Also note channel 2 corresponds to the horizontal movement of first floor, and this will be the same in all transmissibility notations hereinafter. Fourier transform is adopted to transform the measured data from time domain to frequency domain. From Fig. 4, transmissibility T (5, 3) shows a clear difference between State #1 and State #6, while little difference exists between State #1, State #2 and State #10. It might be concluded that the added mass at the base and small nonlinearity induced by the bumper do not generate sufficient change in the response compared with that caused by the stiffness reduction in the column '2BD'. And this challenges detecting the structural damages directly from transmissibility solely. Note that same phenomenon appear in T(4, 3) in Fig. 5, which implies the necessity of enhancement for transmissibility in order to achieve the damage detection goal.

For comparison purposes, Figs. 6 and 7 depict FRF (5, 1) and FRF (4, 1), respectively. Note FRF (5, 1) herein means the FRF between channel 5 and channel 1, channel 1 means the excitation signal. The notation here also follows the same as transmissibility illustrated above. From both figures, some differences can be found in [60,80] Hz between State #1, State 2 and State 6. While for State #10, i.e. minor nonlinearity, little difference exists except in the high frequency domain beyond 100 Hz. It should be noted that high frequency domain is easily influenced by environmental noise, thus it is not good to select for separating different states. From this starting point, it would also be desirable to have further investigation in order to unveil the small differences hidden between these damaged states and the baseline state.

Comparing Figs. 6 and 7 with Figs. 4 and 5, one may find that the FRFs in Figs. 6 and 7 have a better performance at some level in recognizing the small difference between the baseline and the considered states since FRF (5, 1) and FRF (4, 1), can also detect State #2, while transmissibility T (5, 3) and T(4, 3) both fail at this discrimination. However, the drawback of requiring the

Table 2
Structural state condition [40].

Label	State condition	Case description
State #1	Undamaged	Baseline condition
State #2	Undamaged	Added mass (1.2 kg) at the base
State #3	Undamaged	Added mass (1.2 kg) at the first floor
State #4	Undamaged	Stiffness reduction in column 1BD
State #5	Undamaged	Stiffness reduction in column 1AD and 1BD
State #6	Undamaged	Stiffness reduction in column 2BD
State #7	Undamaged	Stiffness reduction in column 2AD and 2 BD
State #8	Undamaged	Stiffness reduction in column 3BD
State #9	Undamaged	Stiffness reduction in column 3 AD and 3 BD
State #10	Damaged	Gap (0.2 mm)
State #11	Damaged	Gap (0.15 mm)
State #12	Damaged	Gap (0.13 mm)
State #13	Damaged	Gap (0.10 mm)
State #14	Damaged	Gap (0.05 mm)
State #15	Damaged	Gap (0.2 mm) and mass (1.2 kg) at the base
State #16	Damaged	Gap (0.2 mm) and mass (1.2 kg) on the 1st floor
State #17	Damaged	Gap (0.1 mm) and mass (1.2 kg) on the 1st floor

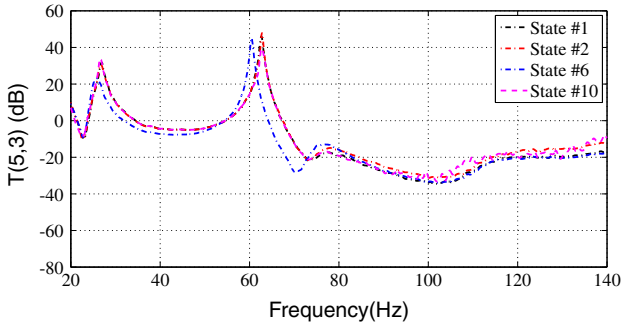

Fig. 4. Transmissibility T(5, 3) for States #1, #2, #6 and #10.

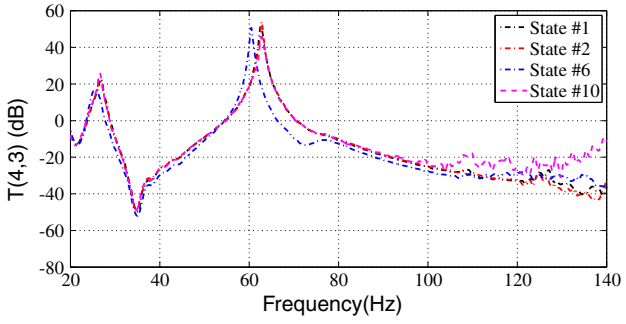

Fig. 5. Transmissibility T(4, 3) for States #1, #2, #6 and #10.

measurement of excitation will largely restrict the widespread application of FRF in real engineering.

4.2.2. Damage detection using CI

The frequency band selection is an arduous task, which may highly affect the results of final detection. In previous investigations [11,12,22,28,34], this point has been highlighted and emphasized with some case studies, while no clear rule has been drawn out. The selection still relies on the experience of engineer, which may differ from one to another.

Figs. 8 and 9 illustrate CI (5, 2) and CI (5, 3) with R = 1, 2, 3 and 4 under selected frequency band [20,100] Hz for State #1-#17, respectively. Note that each state has 50 measurements, and then in total for all 17 states, 850 measurements exist. For instance, in

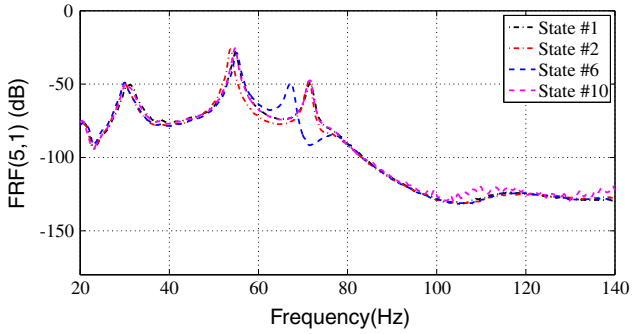

Fig. 6. FRF (5, 1) for States #1, #2, #6 and #10.

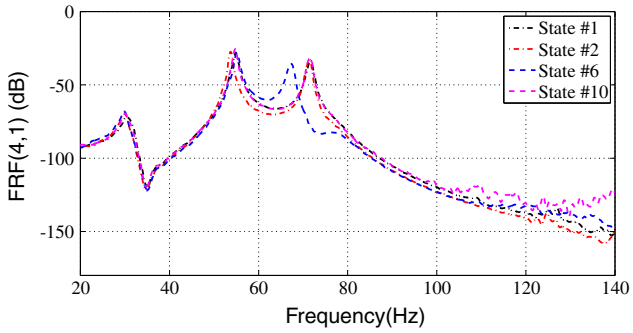

Fig. 7. FRF (4, 1) for States #1, #2, #6 and #10.

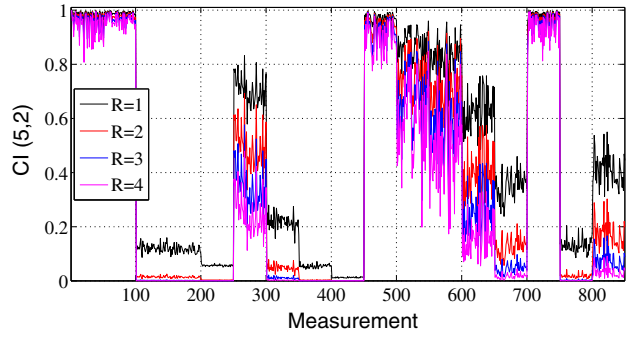

Fig. 8. CI(5, 2) for States #1 to #17 in frequency band [20,100] Hz.

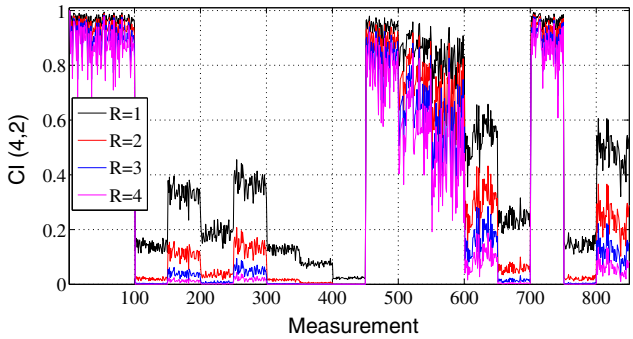

Fig. 9. CI(4, 2) for States #1 to #17 in frequency band [20,100] Hz.

Fig. 8, the horizontal axis draws the number of measurements, i.e. measurements 1–50 represent the State #1, and measurements 51 to 100 represent State #2, . . ., measurements 801 to 850 represent State #17. In those figures hereafter, this holds the same. From

both figures, one can clearly find the difference between baseline State #1 and other states except State #2. For State #3 to State #17, CI (5, 2) and CI (5, 3) successfully detect the changes compared with baseline, i.e. mean damages. However, for State #2, both CI (5, 2) and CI (5, 3) failed in the detection of adding mass to the base. This might insinuate that frequency band might be reselected or optimized. As R increases from '1' to '4', the CI (5, 2) and CI (4, 2) drop more than the previous ones. This suggests that the higher the R is, the more sensitive it performs. However, there should be a compromise between the sensitivity and noise tolerance, while the higher the R is, the less noise it can tolerate. If little noise would harm the results at a high level, then it would be vague in the engineering application. This will be further discussed in the latter analysis hereinafter.

Figs. 10 and 11 illustrate the CI (5, 4) and CI (4, 3) for R = 1, 2, 3, and 4 in frequency band [100,140] Hz for States #1 to #17. Form these two figures, both CI (5, 4) and CI (4, 3) show obvious change between baseline and States #2 to #17. This means that damages are successfully detected. One can also find that: (i). For State #2, it might be not well detected if R = 1, but if selecting R = 2, 3, or 4, then it would be pretty obvious; (ii). As R increases from '1' to '4', CI (5, 4) and CI (4, 3) give more sensitive predictive results for damages. (iii). For quantifying each state, it might be challenging in drawing out any conclusion since the difference between each state is not quite distinct.

Comparing Figs. 10 and 11 with Figs. 8 and 9, one can find that (i). CI (5, 2) and CI (4, 2) give more distinct separation between States #3 to #17, while CI (5, 4) and CI (4, 3) successfully detect State #2, but fail in separating the states from each other; (ii). The combination of CIs from different frequency band might give a better strategy of damage detection.

Figs. 12 and 13 illustrate CI (5, 1) and CI (4, 1) in frequency band [20, 100] Hz with R = 1, 2, 3, and 4 for States #1 to #17. From these two figures, one can find that: (i). All damages are successfully identified from the baseline as clear difference can be found between States #2 to #17 from the baseline State #1; (ii). As R increases from '1' to '4', CI (5, 1) and CI (4, 1) show more sensitive performance; (iii). Since difference between each state also exists, this implies that CI (5, 1) and CI (4, 1) might also be adopted to quantify the damage in a relative way.

Comparing Figs. 12 and 13 of FRF based CIs with Figs. 8, 9, 10 and 11 of transmissibility based CIs, one can find that: (i). With the same frequency band [20,100] Hz, transmissibility based CIs of Figs. 8 and 9 do not perform well as FRF based CIs of Figs. 12 and 13, which does not mean that FRF based CI will be always better than transmissibility based CI. For instance, under [100, 140] Hz, transmissibility based CI can successfully detect damage in State #2, while FRF based CI fail in detecting more damages as shown in Fig. 14; (ii). For both transmissibility and FRF based CI, the selection of the value of R is also an important task, certainly the higher it is chosen, the more sensitive the CI will be. However, one should also bear in mind the compromise for noise tolerance.

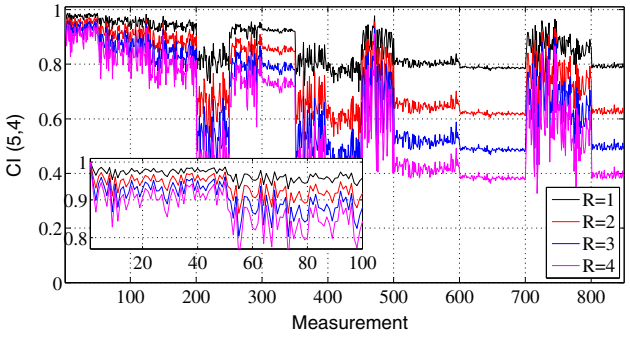

Fig. 10. CI(5, 4) for States #1 to #17 in frequency band [100,140] Hz.

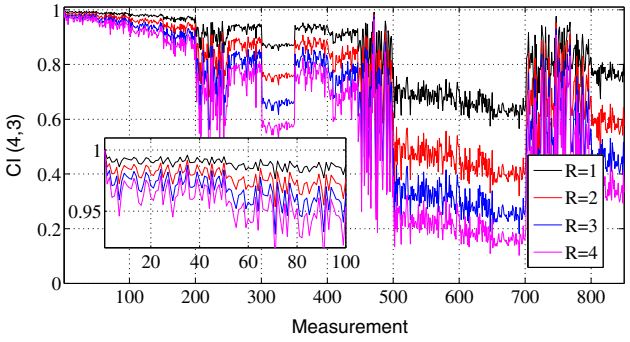

Fig. 11. CI(4, 3) for States #1 to #17 in frequency band [100,140] Hz.

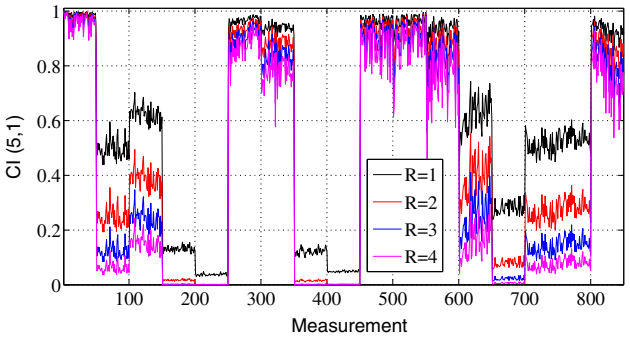

Fig. 12. CI(5, 1) for States #1 to #17 in frequency band [20,100] Hz.

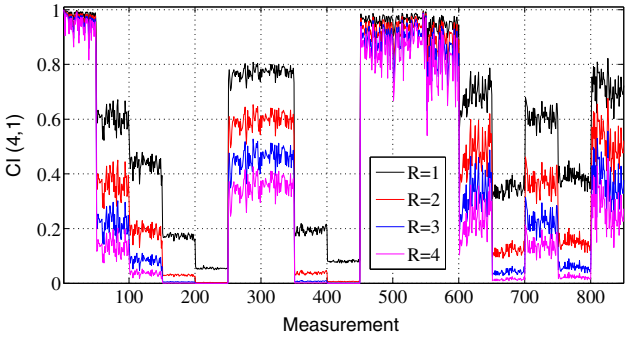

Fig. 13. CI(4, 1) for States #1 to #17 in frequency band [20, 100] Hz.

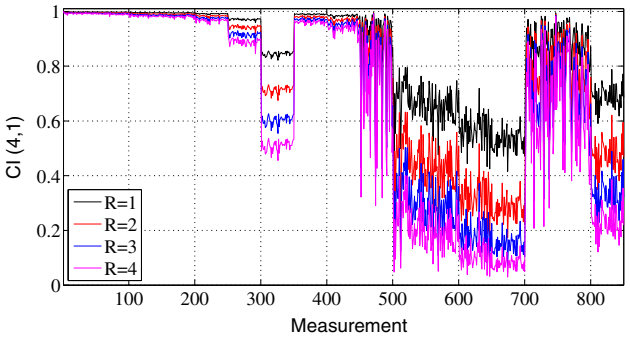

Fig. 14. CI(4, 1) for States #1 to #17 in frequency band [100, 140] Hz.

4.2.3. Damage detection using ETDI

Figs. 15 and 16 illustrate transmissibility based ETDI with $Q = 1$, 2, 3, 4, and $Q = 1$, 6, 7, 8, respectively. From both figures, one can find: (i). All damages are successfully detected from the baseline, while for $Q = 1$, it will be challenging to detect in State #2, for $Q = 2$, 3, and higher values, State #2 is detected for all cases; (ii). The higher the value chosen for Q is, the more sensitive ETDI will be in detecting the damages; (iii). Since all states vary different from each other, it might suggest that ETDI can also be used to relatively quantify the damages, while $Q = 1$ is not a good choice, a higher value might be much better, e.g. $Q = 2$ will be enough. This agrees well with MAC. Certainly one may set a higher value for Q in the light of the actual application.

Figs. 17 and 18 show FRF based ETDI for $Q = 1$, 2, 3, 4 and $Q = 1$, 6, 7, 8, respectively. From these two figures, one can find that: (i). For $Q = 1$, ETDI either fails to detect it; while for $Q > 1$, ETDI can detect State #2; (ii). As Q increases from '1' to '8', the higher the value of Q is, the more sensitive the ETDI will be; (iii). Similar to transmissibility based ETDI, FRF based ETDI also vary clearly between each state. This might also suggest that it can be used for further relatively quantifying structural damage.

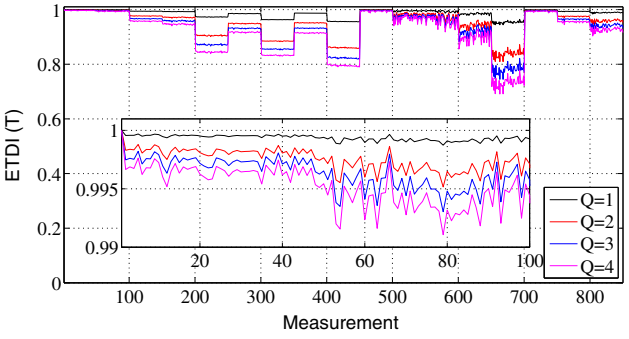

Fig. 15. Transmissibility based ETDI for States #1 to #17 with $Q = 1$, 2, 3, 4.

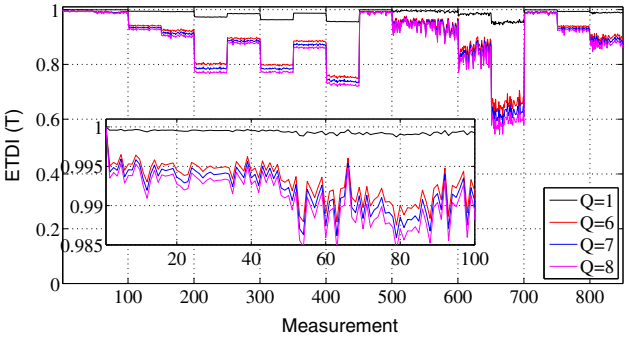

Fig. 16. Transmissibility based ETDI for States #1 to #17 with $Q = 1$, 6, 7, 8.

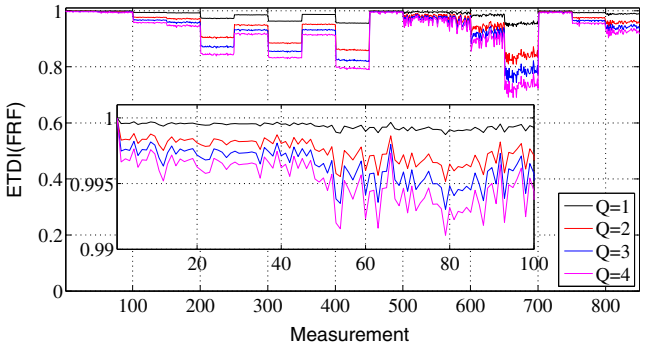

Fig. 17. FRF based ETDI for States #1 to #17 with $Q = 1$, 2, 3, 4.

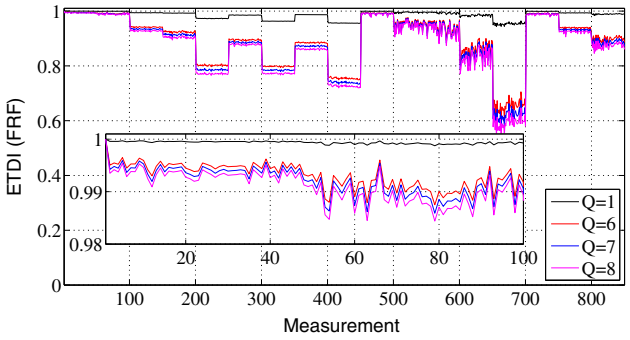

Fig. 18. FRF based ETDI for States #1 to #17 with $Q = 1$, 6, 7, 8.

Comparing Figs. 17 and 18 with Figs. 15 and 16, it can be concluded that: (i). Both transmissibility based ETDI and FRF based ETDI are effective in damage detection, and as Q increases, the ETDI will be more sensitive, while the Q value setting depends on the engineer's experience; (ii). For $Q > 1$, ETDI might be used to quantify structural damages at a relative scale.

5. Concluding remarks

This study summarized a damage detection strategy using transmissibility incorporated with cosine measure and MAC, while unveils the interrelation between them since previous investigations normally employ them separately. And this study also defines two new damage indicators, namely cosine based indicator (CI) at the basis of previous indicator cosine measure and MAC, and extended transmissibility damage indicator ETDI based on previous indicator TDI. Finally a three-story benchmark structure is adopted to verify the proposed damage detection strategy. The concluding remarks can be summarized as follows:

(1) The CI and ETDI are both effective in damage detection, and as their power values R and Q increase, they become more sensitive in detecting damage. However, the more sensitive they are, the less tolerance they will hold to the environmental uncertainty. The setting of the R and Q values is empirical and depends on the engineer's experience; for instance, one may set them as 2 as initial tests, if not achieving required performance, to increase it will later fulfill the criterions set. Certainly this depends on the engineering experience and as case dependent and empirical setting, it will vary in accordance to different applications.

(2) CI only requires measurement from two nodes, and taking one frequency band in further analysis, which might give an efficient estimation for damage compared with ETDI that takes the whole frequency band. Note that CI demands engineer's experience in frequency band selection, while ETDI has no restriction, which provide a simple application.

(3) As to damage quantification, both CI and ETDI show potential in relative quantification manner, while for general application in complex structures, further investigation is needed.

Acknowledgement

The first author thanks CWO (Commissie Wetenschappelijk Onderzoek), Faculty of Engineering and Architecture, Ghent University for providing financial support for a research stay at Soete Laboratory.

References

[1] Sohn H, Farrar CR, Hemez FM, Shunk DD, Stinemates SW, Nadler BR and Czarnecki JJ 2004 A review of structural health monitoring literature from 1996–2001 Technical Report LA-13976-MS Los Alamos National Laboratory.

[2] Montalvao D, Maia NMM, Ribeiro AMR. A review of vibration-based structural health monitoring with special emphasis on composite materials. Shock Vibr Digest 2006;38(4):295–324.

[3] Zhou Y-L, Maia NMM, Sampaio R, Wahab MA. Structural damage detection using transmissibility together with hierarchical clustering analysis and similarity measure. Struct Health Monit 2016. http://dx.doi.org/10.1177/1475921716680849.

[4] Khatir S, Belaidi I, Serra R, Abdel Wahab M, Khatir T. Numerical study for single and multiple damage detection and localization in beam-like structures using BAT algorithm. J Vibroeng 2016;18(1):202–13.

[5] Khatir A, Tehami M, Khatir S, Abdel Wahab M. Multiple damage detection and localization in beam-like and complex structures using co-ordinate modal assurance criterion combined with firefly and genetic algorithms. J Vibroeng 2016;18(8):5063–73.

[6] Gillich G-R, Praisach Z-I, Abdel Wahab M, Gillich N, Mituletu IC, Nitescu C 2016 Free vibration of a perfectly clamped-free beam with stepwise eccentric distributed masses Shock and Vibration 2016(Article ID 2086274) 10 pages; doi: 10.1155/2016/2086274.

[7] Khatir S, Belaidi I, Serra R, Abdel Wahab M, Khatir T. Damage detection and localization in composite beam structures based on vibration analysis. Mechanika 2015;21(6):472–9.

[8] Maia NMM, Urgueira APV, Almeida RAB. Whys and Wherefores of Transmissibility Vibration Analysis and Control – New Trends and Developments. InTech; 2011. ISBN 978-953-307-433-977, 364 pages, pp. 197–216.

[9] Maia NMM, Lage YE, Neves MM. Recent Advances on Force Identification in Structural Dynamics Advances in Vibration Engineering and Structural Dynamics. InTech; 2012. ISBN 978-953-951-0845-0840, 0378 pages, pp. 0103–0132.

[10] Chesne S, Deraemaeker A. Damage localization using transmissibility functions: a critical review. Mech Syst Signal Process 2013;38(2):569–84.

[11] Zhou YL. Structural health monitoring by using transmissibility PhD thesis, 2015.

[12] Zhou Y-L, Maia NMM, Wahab MA. Damage detection using transmissibility compressed by principal component analysis enhanced with distance measure. J Vib Control 2016. http://dx.doi.org/10.1177/1077546316674544.

[13] Allemang RJ, Brown DL, A Correlation Coefficient for Modal Vector Analysis Proceedings of the 1st International Modal Analysis Conference, 1982, 110–116.

[14] Allemang RJ. The Modal Assrance Criterion (MAC): Twenty Years of Use and Abse Journal of Sound and Vibration August 14–21, 2003.

[15] Pascal R, Golinval JC, Razeto M. A Frequency Domain Correlation Technique for Model Correlation and Updating Proceedings of the 15th International Modal Analysis Conference – IMAC 587–592, 1997.

[16] Heylen W, Lammens S, Sas P. Modal Analysis Theory and Testing KU Leuven-PMA Belgium, Section A.6, 1998.

[17] Maia NMM, Ribeiro AMR, Fontul M, Montalvao D, Sampaio RPC. Using the detection and relative damage quantification indicator (DRQ) with transmissibility. In: Garibaldi L, Surace C, Holford K, Ostachowicz WM, editors. Damage Assessment of Structures Vii. Key Engineering Materials. 3472007. p. 455–460.

[18] Perera R, Ruiz A, Manzano C. An evolutionary multiobjective framework for structural damage localization and quantification. Eng Struct 2007;29:2540–50.

[19] Sampaio R, Maia N. Strategies for an efficient indicator of structural damage. Mech Syst Signal Process 2009;23:1855–69.

[20] Perera R, Ruiz A, Manzano C. Performance assessment of multicriteria damage identification genetic algorithms. Comput Struct 2009;87:120–7.

[21] Zhou YL, Perera R, Sevillano E. Damage identification from power spectrum density transmissibility Proceedings of the 6th European Workshop on Structural Health Monitoring Dresden, Germany, July 2012, 2012.

[22] Zhou Y-L, Figueiredo E, Maia NMM, Perera R. Damage detection and quantification using transmissibility coherence analysis Shock and Vibration 2015(Article ID 290714), 2015.

[23] Sampaio R, Maia N, Almeida RAB, Urgueira APV. A simple damage detection indicator using operational deflection shapes. Mech Syst Signal Process 2015;72–73:629–41.

[24] Zhou Y-L, Wahab MA. Rapid early damage detection using transmissibility with distance measure analysis under unknown excitation in long-term health monitoring. J Vibroeng 2016;18(7):4491–9.

[25] Santos FLM, Peeters B, Auweraer H, Goes LCS and Desmet W, Vibration-based damage detection for a composite helicopter main rotor blade Case studies in Mechnical Systems and Signal Processing 3(22–27), 2016.

[26] Zhou Y-L, Wahab MA, Perera R. Damage detection by transmissibility conception in beam-like structures. Int J Fract Fatigue Wear 2015;3:254–9.

[27] Zhou YL, Perera R. Transmissibility based damage assessment by intelligent algorithm Proceedings of the 9th European Conference on Structural Dynamics (EURODYN 2014) Oporto, Portugal, June 2014, 2014.

[28] Zhou Y-L, Wahab MA, Figueiredo E, Maia NMM, Sampaio R, Perera R. Single side damage simulations and detection in beam-like structures. J Phys: Conf Ser 2015;628:012036.

[29] Ye J. Cosine similarity measures for intuitionistic fuzzy sets and their applications. Math Comput Model 2011;53:91–7.

[30] Junjie Wua SZ, Liu Hongfu, Xia Guoping. Cosine interesting pattern discovery. Inf Sci 2012;184:176–95.

[31] Liu W, Chen B, Swartz RA, Investigation of Time Series Representations and Similarity Measures for Structural Damage Pattern Recognition The Scientific World Journal 2013 Article ID 248349, 248313 pages, 2013.

[32] Ye J. Improved cosine similarity measures of simplified neutrosophic sets for medical diagnoses. Artif Intell Med 2015;63:171–9.

[33] Xia P, Zhang L, Li F. Learning similarity with cosine similarity ensemble. Inf Sci 2015;307:39–52.

[34] Zhou Y-L, Maia NMM, Sampaio R, Wahab MA, Structural damage detection using transmissibility together with hierarchical clustering analysis and similarity measure. Struct Health Monit Int J, in press, https://dx.doi.org/10.1177/1475921716680849.

[35] Zhou Y-L, Maia NMM, Sampaio R, Qian XD, Wahab MA. Damage detection via transmissibility enhanced with similarity analysis and principal component analysis. In: Proceedings of the 2016 Leuven Conference on Noise and Vibration Engineering (ISMA 2016) Leuven, Belgium, September 2016, 2016.

[36] Zhou Y-L, Figueiredo E, Maia NMM, Sampaio R, Perera R. Damage detection in structures using a transmissibility-based Mahalanobis distance. Struct Control Health Monit 2015;22:1209–22.

[37] Zhou Y-L, Figueiredo E, Maia NMM, Perera R. Damage detection using transmissibility coherence Proceedings of the International Conference on Structural Engineering Dynamics (ICEDyn 2015) Lagos, Algarve, Portugal, June 2015, 2015.

[38] Worden K, Manson G, Fieller NRJ. Damage detection using outliner analysis. J Sound Vib 2000;229(3):647–67.

[39] Figueiredo E, Cross E. Linear approaches to modeling nonlinearities in long-term monitoring of bridges. J Civ Struct Health Monit 2013;3(3):187–94.

[40] http://www.lanl.gov/projects/national-security-education-center/engineering/ei-software-download/thanks.php.

[41] Figueiredo E, Park G, Figueiras J, Farrar CR, Worden K. Structural health monitoring algorithm comparisons using standard data sets Los Alamos National Laboratory Report LA-14393 Los Alamos National Laboratory, 2009.

[42] Figueiredo E. Damage Identification in Civil Engineering Infrastructure under Operational and Environmental Conditions PhD thesis Porto University, Portugal, 2010.

[43] Figueiredo E, Flynn E. Three-story building structure to detect nonlinear effects, 2013 http://wwwlanlgov/projects/national-security-education-center/engineering/ei-software-download/thanksphp.